



Optical coherence tomography in optic disc drusen

J. Alexander Fraser^{1,2}, Lulu L. C. D. Bursztyn^{1,2}

¹Department of Clinical Neurological Sciences, ²Department of Ophthalmology, Western University, London, ON, Canada

Contributions: (I) Conception and design: All authors; (II) Administrative support: None; (III) Provision of study materials or patients: None; (IV) Collection and assembly of data: None; (V) Data analysis and interpretation: None; (VI) Manuscript writing: All authors; (VII) Final approval of manuscript: All authors.

Correspondence to: J. Alexander Fraser, MD. Room B7-104, London Health Sciences Centre, University Hospital, 339 Windermere Road, London, ON N6A 5A5, Canada. Email: alex.fraser@lhsc.on.ca.

Abstract: Optic disc drusen (ODD) are hyaline deposits in the optic nerve head, occurring in approximately 2% of the population. ODD may be superficial and visible, or buried and either invisible or seen only as elevation of the optic disc, mimicking optic disc edema. Advanced optic nerve imaging, including optical coherence tomography (OCT) can be used to diagnose and characterize ODD with very high resolution. Enhanced depth imaging (EDI-OCT) in particular has emerged as the optimal modality to directly visualize ODD. This modality has led to a greater ability to differentiate ODD from optic disc edema and prevent misdiagnosis or invasive testing. We review the characteristic findings of ODD on OCT, their distinguishing features, and the use of OCT as a biomarker in the neuro-ophthalmic assessment of ODD.

Keywords: Drusen; optic disk; tomography; optical coherence

Received: 05 September 2019; Accepted: 11 December 2019; Published: 15 March 2020.

doi: 10.21037/aes.2019.12.03

View this article at: <http://dx.doi.org/10.21037/aes.2019.12.03>

Optic disc drusen (ODD) are rounded, calcified, concentrically laminated hyaline deposits situated in the prelaminar tissue of the optic nerve. Though they are predominantly dense nuggets of calcium phosphate, $\text{Ca}_3(\text{PO}_4)_2$, ODD also contain mucopolysaccharides, glycoproteins, amino acids, and nucleic acids (1-3). Optically, ODD are glassy and translucent; they autofluorescence (4) but are not birefringent (5). Although most patients with ODD are asymptomatic, visual field loss is common, occurring in up to 50% of children and 87% of adults (6). As there is no known prevention of or treatment for ODD, the primary clinical relevance of ODD is their tendency to mimic optic disc edema.

Modalities for evaluating ODD

Ophthalmoscopy

Superficial ODD are evident during ophthalmoscopy as bright lumpy refractile bodies shimmering within the substance of the optic disc (7). ODD that are not superficial

are called “buried”; though they may sometimes betray their presence by causing non-edematous optic disc elevation, more often they do not affect the ophthalmoscopic appearance of the optic disc at all. In the general population, superficial ODD have a prevalence of 0.2–0.3% (8,9), but cadaveric and enucleated histopathological specimens reveal a much higher prevalence of combined superficial and buried ODD, at 1.8–2.0% (3,10). Ophthalmoscopy and fundus photography are therefore insensitive tools for detecting and assessing ODD, particularly buried ODD.

Ultrasound, CT, fundus autofluorescence

Before the era of OCT, more conventional imaging modalities were used to detect buried ODD, with varying degrees of sensitivity (*Figure 1*). B-scan orbital ultrasonography was, for many years, considered the gold-standard modality for ODD evaluation and shown to be more reliable than other contemporaneous modalities, such as fundus autofluorescence imaging or high-resolution orbital computed tomography (CT) (11). For example, in

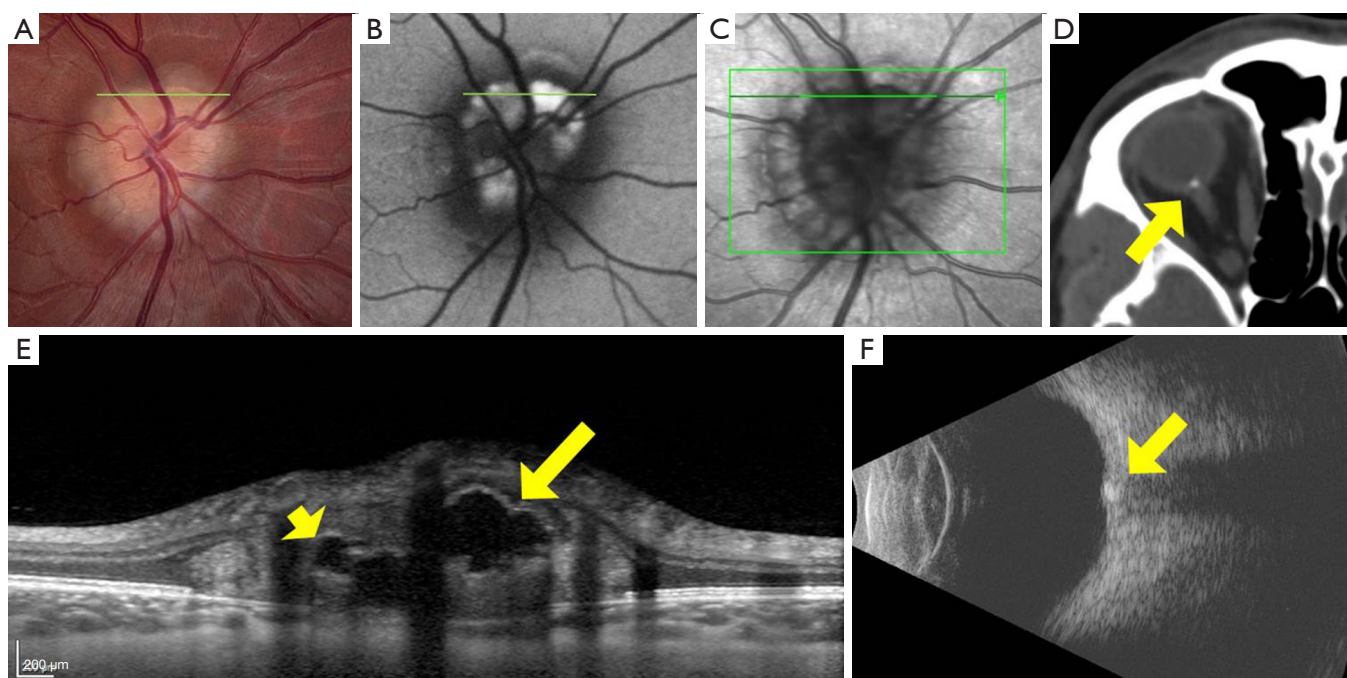


Figure 1 Comparison of different imaging modalities for ODD: (A) fundus photograph showing a superficial ODD at the 1 o'clock position and non-edematous optic disc elevation elsewhere suggestive of underlying buried ODD; (B) fundus autofluorescence imaging showing brightly autofluorescing ODD; (C) infrared photograph for OCT planning; (D) computed tomography (CT) orbits showing ODD as a single hyperdense calcified deposit at the level of the optic disc (arrow); (E) EDI-OCT, at the section indicated by the green line in panels A, B, and C, showing detailed cross-sectional view of the optic disc, containing superficial (long arrow) and more deeply buried (short arrow) ODD; (F) B-scan orbital ultrasound showing ODD as a single echogenic focus in the optic disc (arrow). ODD, optic disc drusen.

one study of 82 eyes with suspected ODD, autofluorescence detected ODD in 15 eyes, while ultrasonography detected ODD in 39 (and did not miss any of the ODD detected by FAF or by CT) (11).

OCT

The first report of OCT in the evaluation of ODD was published in 1998 (12), and showed that, compared to age-matched controls, patients with ophthalmoscopically visible ODD had significant thinning of the peripapillary retinal nerve fiber layer (RNFL) on time-domain OCT. This report also included the first OCT image of an ODD, visible as a signal-poor (dark) deposit within the optic disc, causing elevation of the optic nerve head (12). With the advent of spectral-domain OCT (SD-OCT) in the mid-2000s, scanning time decreased and image resolution increased remarkably; SD-OCT could not just detect ODD, but could pinpoint their location, shape, volume, and number with newfound accuracy (13). The

appearance of ODD on SD-OCT was initially described as one of a signal-poor core with a hyperreflective anterior border, like a superficial “cap” (13,14); however, even after this important imaging advance, the posterior borders of ODD and deeper structures in the prelaminar optic nerve remained indistinct or invisible using first-generation SD-OCT techniques, owing to poor penetration.

Technological advances in OCT

Two subsequent developments independently allowed deeper penetration of optic disc tissue and better visualization of ODD posterior borders; the first was enhanced-depth-imaging OCT (EDI-OCT), and the second was swept-source OCT (SS-OCT) (15,16). EDI-OCT is a modification of standard SD-OCT technique, that shifts the coherence gate of the OCT apparatus to deeper structures in the eye, enhancing their visibility and resolution (17). While EDI-OCT can be performed using a standard SD-OCT machine (containing a low-coherence

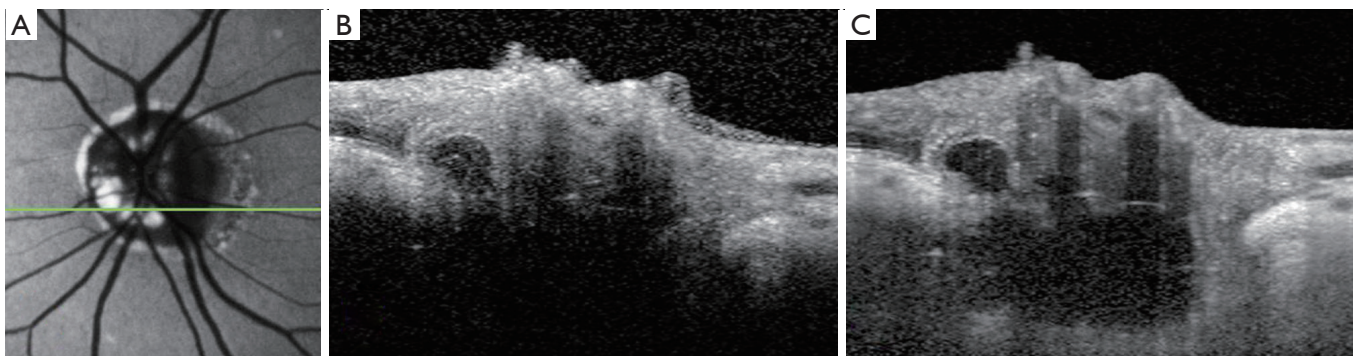


Figure 2 Comparison of non-EDI SD-OCT *vs.* EDI-OCT: (A) fundus autofluorescence imaging of a patient with ODD, green line indicating the level of the OCT cross-sections; (B) non-EDI-OCT, showing anterior optic disc structures, including a single superficial ODD, but indistinct or invisible structures more posteriorly; (C) EDI-OCT, showing deep structures, including the anterior and posterior surfaces of a large buried ODD with its adjacent hyperreflective bands, and better definition of more anterior optic disc structures, including the superficial ODD seen in panel (B). EDI, enhanced depth imaging; SD-OCT, spectral-domain optical coherence tomography; ODD, optic disc drusen.

broad-bandwidth light source), SS-OCT requires a high-coherence laser light source that can sweep across different wavelengths, and therefore necessitates different equipment. Because longer wavelengths of light are used in SS-OCT than standard SD-OCT, deeper penetration of ocular tissue is possible without scatter (15). Both EDI-OCT and SS-OCT can penetrate to the level of the lamina cribrosa, much deeper than the limit of standard SD-OCT, and appear equally suited to imaging the hyperreflective posterior borders of ODD and more deeply buried ODD (Figure 2) (15,16). Software algorithms can now be used to calculate ODD volumes based on SS-OCT (18) or EDI-OCT (19,20) data and even render 3-dimensional rotatable visual representations of ODD.

In an influential 2013 study, Merchant and colleagues prospectively compared EDI-OCT to non-EDI SD-OCT and B-scan orbital ultrasound in a series of 68 eyes (32 with definite superficial ODD on ophthalmoscopy, 25 with suspected buried ODD, and 11 normal-appearing optic discs) (21). The EDI-OCT correlate of a definite superficial ODD was, in all cases, a rounded mass with a signal-poor core, surrounded by short hyperreflective bands perpendicular to the OCT beam (Figure 3). All such eyes also had isolated or clustered hyperreflective bands *without* an associated signal-poor core elsewhere in the optic disc. Taking these features to be the OCT “signatures” of ODD, the authors identified ODD in 17 of the 25 suspected ODD cases on EDI-OCT (*vs.* 14 for non-EDI-OCT and *vs.* 7 for B-scan orbital ultrasound), and 3 of the 11 normal cases on

EDI-OCT (*vs.* 1 for non-EDI-OCT and *vs.* 1 for B-scan orbital ultrasound). Overall, the authors found that EDI-OCT was superior to the other modalities: it detected ODD more often than non-EDI-OCT or B-scan orbital ultrasound, and it did not miss any of the ODD detected by these other modalities. In a later study, EDI-OCT was also found to be superior to fundus autofluorescence imaging at detecting ODD, particularly smaller or more deeply buried ODD (22).

Other OCT modalities in the evaluation of ODD

RNFL analysis

Although OCT can be used to image ODD directly, it can also be used to assess their indirect influence on other structures in the retina. RNFL thickness, a surrogate for axonal integrity within the optic nerve, has been a consistent target of OCT measurement since the first time-domain OCT publications of the late 1990s, and has repeatedly shown attenuation correlating with increased ODD size and superficiality on time-domain OCT (12,23,24) and SD-OCT (19,24-26). This attenuation was not evident in a cohort of children with ODD, suggesting that loss of RNFL thickness occurs as a result of damage over time (27). One advantage of OCT (and RNFL analysis in particular) over traditional modalities for ODD assessment is the ability to correlate ODD burden with degree of neuroaxonal injury or functional correlation with visual outcomes. Moreover, structural and quantitative analysis of ODD by OCT allows

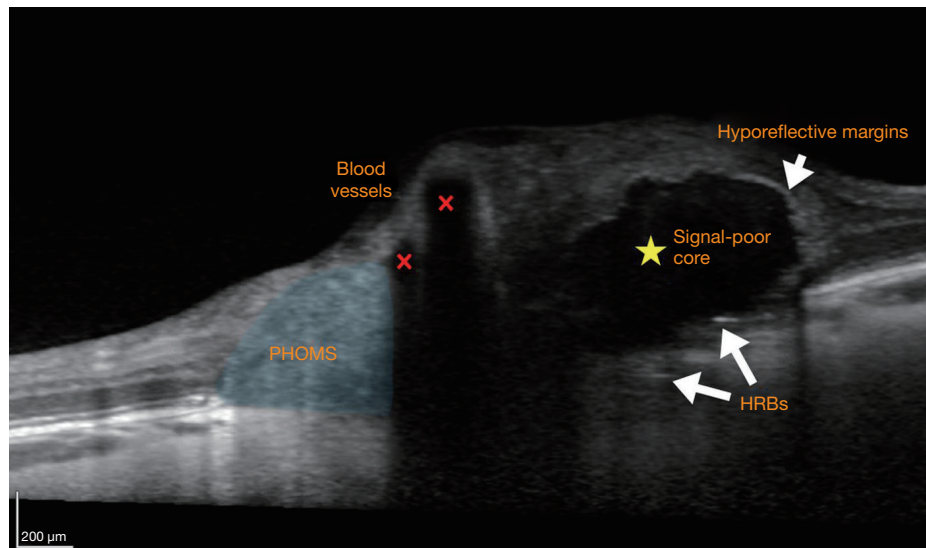


Figure 3 Characteristics of ODD and other structures on EDI-OCT: Large superficial ODD (yellow star), identifiable as a mass with a signal-poor (dark, hyporeflexive) core and hyperreflective margins (short arrow); horizontal hyperreflective bands (HRBs) are evident along the posterior margins of the ODD (long arrows). Two blood vessels (red X) appear adjacent to each other and cast long shadows on the deeper structures. A peripapillary hyperreflective ovoid mass-like structure (PHOMS), representing the anterolateral herniation of axons is evident lateral to the scleral canal in the peripapillary region (blue shading). ODD, optic disc drusen; EDI-OCT, enhanced depth imaging optical coherence tomography.

for correlation of clinically relevant measures of visual function over time.

GCIPL analysis

Macular ganglion cell-inner plexiform layer (GCIPL) OCT has also shown thinning corresponding to ODD severity (25). Because GCIPL thinning seems to correlate with the presence of deeper ODD better than RNFL thinning does, GCIPL analysis may be better for detecting earlier structural damage associated with deeply buried ODD than RNFL analysis (25).

OCT-A

OCT angiography (OCT-A) is a novel means of imaging the microvasculature of the retina and segmenting it by layer. Unlike fluorescein angiography, it is non-invasive and can achieve micrometer precision, but has not been widely studied in ODD. Central retinal vascular anomalies, including cilioretinal arteries, retinochoroidal collateral vessels, increased vascular tortuosity and early branching, are frequently associated with ODD (28,29). OCT-A is a promising modality to better characterize these differences.

In one report of a patient with superficial ODD, OCT-A showed focal loss of capillaries in the superficial laminar segment overlying the most prominent ODD, in addition to a focal thinning of the RNFL corresponding to the distribution of the ODD (30). A subsequent study of 19 eyes with ODD showed lower flow index and vessel density on OCT-A compared to normal eyes. These OCT-A abnormalities were found to correlate with GCIPL abnormalities, but not with RNFL parameters (31).

OCT: diagnosing ODD in the modern imaging era

In 2018, the Optic Disc Drusen Studies (ODDS) Consortium published “Recommendations for Diagnosis of ODD using OCT” in an effort to standardize the OCT diagnosis of ODD (32). This international working group of experts published their consensus regarding the OCT acquisition and diagnosis of ODD. Reviewing the literature, the consortium came to the opinion that EDI-OCT was to be considered the most reliable imaging method for assessing ODD. The consortium outlined the recommended acquisition protocol to achieve standardization for future research (*Table 1*). Then, using an iterative multi-step review process of 74 individual EDI-OCT data sets, the

Table 1 Recommended scanning protocol from Optic Disc Drusen Studies (ODDS) Consortium

Acquisition
Dilate pupils before examination if necessary
Use SD-OCT in EDI mode
If no SD-OCT is available, adjust the distance from the OCT apparatus to the eye to get an inverted view of the optic nerve head for better visualization of deeper structures
Dense optic nerve head scan
Select high-resolution acquisition if possible
Centre a scan area of 15° × 10° over the optic disc
Scan with 97 sections in that area (30 μm between each scan)
Average at least 30 frames
Perform the volume scan in both horizontal and vertical directions

Adapted with permission from Malmqvist *et al.* (32). EDI, enhanced depth imaging; OCT, optical coherence tomography; SD-OCT, spectral-domain optical coherence tomography.

group agreed on OCT features diagnostic of ODD as well as common artifacts that they thought should not be considered indicative of ODD.

Characterizing the appearance of ODD

The ODDS Consortium reached a consensus to define ODD as “hyporeflexive structures with a full or partial hyperreflexive margin” (*Figure 3*) (32), in keeping with most of the previously published OCT studies. The hyporeflexive, signal-poor, core of an ODD is a result of its uniform index of refraction and lack of reflective internal optical interfaces. The hyperreflexive outer margins demarcate the sharp optical interface between an ODD and neighboring tissue. Earlier work using non-EDI SD-OCT showed an anterior “cap” sign, initially believed to represent the nidus of calcification from which ODD arise (14). Subsequent EDI-OCT studies have shown that each ODD is enveloped in an outer jacket of hyperreflexivity, even along its posterior border, with an EDI-OCT appearance reminiscent of a dark egg. The apparent “cap” sign anteriorly was simply an artefact of insufficiently deep optical penetration by earlier-generation OCT techniques (*Figure 2*) (16,21).

ODD, when they are detected, are always visualized anterior to the lamina cribrosa (21,32). The leading theory of ODD pathogenesis holds that, in the small scleral canals of ODD patients, the lamina cribrosa acts as a “choke point” for axoplasmic transport, resulting in calcium build-up within intra-axonal mitochondria. These mitochondria

are subsequently extruded into the extracellular space proximal to the obstruction, i.e., anterior to the lamina cribrosa, where they act as niduses for runaway calcium deposition, ultimately growing into ODD (1).

An eye may have only a single ODD, or multiple ODD, and these can be situated at differing depths between the lamina cribrosa and the optic disc surface; ODD may sometimes form conglomerations with other ODD to create more complicated, multilobed, structures (*Figure 4*).

Hyperreflexive bands

Although the hyporeflexive cores of ODD are invariably associated with hyperreflexive bands (21), it is not yet clear what *isolated* hyperreflexive bands (without an associated hyporeflexive core) may represent. Hyperreflexive bands on a single OCT slice may only *seem* isolated until their parent ODD is detected on an adjacent OCT section (*Figure 5*). When truly isolated hyperreflexive bands are seen, however, they are always situated deep in the optic nerve head between the lamina cribrosa and Bruch’s membrane, in a region where OCT image detail becomes degraded (*Figure 4E*). Some researchers have theorized that isolated hyperreflexive bands may represent nascent ODD, that have not yet grown to the number or size required to form a fully mature ODD (21). These hyperreflexive bands do not seem to be an imaging artefact, because they persist in their location and extent when the EDI-OCT scanning protocol is altered (21,33). Nevertheless, the ODDS Consortium has recommended, for now, that isolated hyperreflexive bands

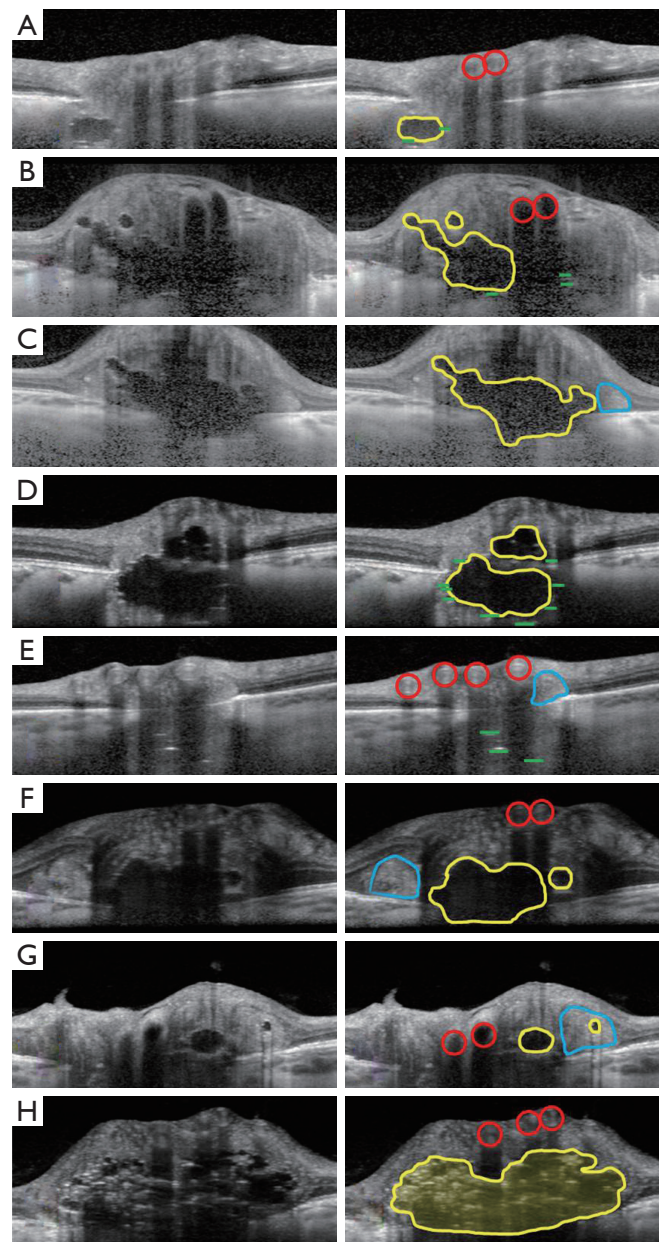


Figure 4 Selected EDI-OCT features in the evaluation of ODD: original (LEFT) and annotated (RIGHT) EDI-OCT images [ODD outlined in yellow; blood vessels outlined in red; horizontal hyperreflective bands (HRBs) highlighted in green; peripapillary hyperreflective ovoid mass-like structures (PHOMS) outlined in blue]. (A) Solitary deeply buried ODD with adjacent HRBs, blood vessels in a sideways “figure-of-eight” configuration; (B) two superficial ODD of different sizes, one of which resembles a blood vessel, but is shown to be a discrete lump on adjacent OCT sections (not shown). Isolated HRBs situated between the lamina cribrosa and Bruch’s membrane; (C) large superficial drusen that extends deep, with an associated PHOMS; (D) multiple ODD, the deep one demonstrating HRBs along its edges and posterior surface; (E) isolated HRBs (not associated with an adjacent ODD). Also shown are blood vessels and a PHOMS; (F) two ODD, the smaller of which resembles the overlying blood vessels (also shown) but does not have a “figure-of-eight” configuration, dark shadowing, or a tubular structure on adjacent OCT sections. Also shown is a PHOMS; (G) two small superficial drusen, one of which is embedded in a PHOMS and therefore likely herniated forward with the other nerve fibers. A pair of blood vessels is also shown; (H) a “conglomeration” of innumerable small superficial ODD (shaded yellow area) with overlying blood vessels. ODD, optic disc drusen; EDI-OCT, enhanced depth imaging optical coherence tomography.

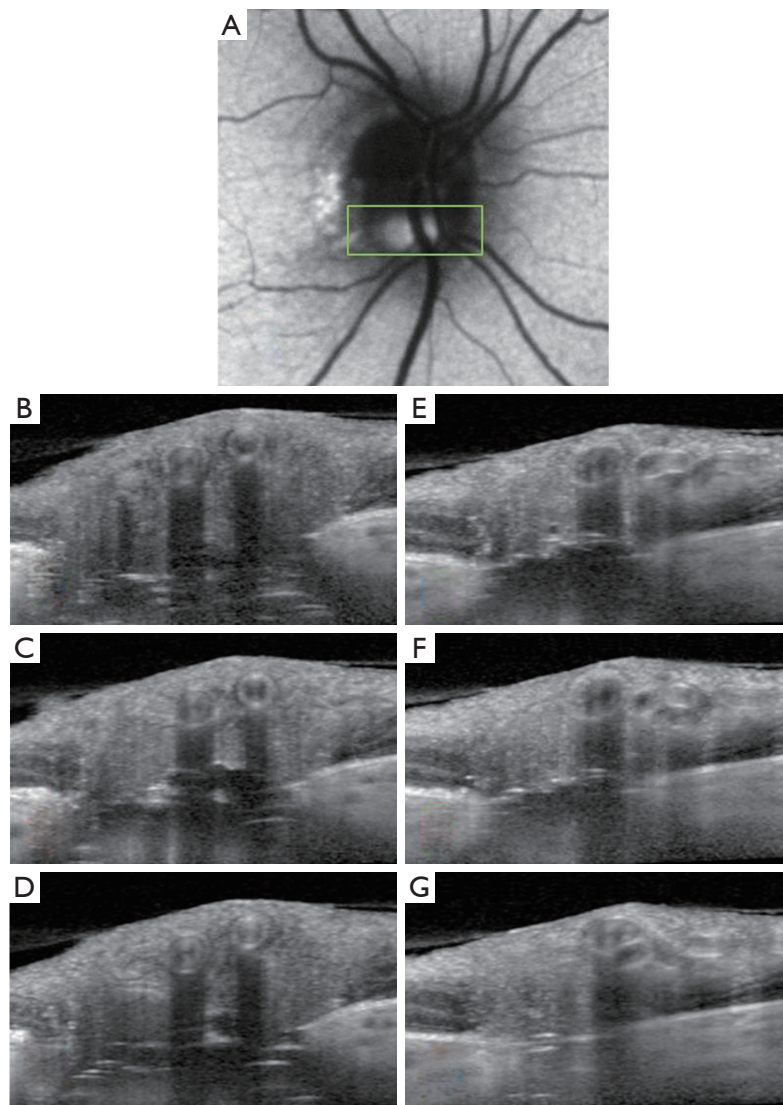


Figure 5 The utility of scrolling through adjacent EDI-OCT images: (A) fundus autofluorescence image of the optic disc showing the region (and hyperfluorescent ODD) scanned by EDI-OCT according to the Optic Disc Drusen Studies (ODDS) Consortium's recommended acquisition protocol (32). Six consecutive parallel horizontal sections were obtained (panels B,C,D,E,F,G), starting at the top of the green box (panel B) and finishing at the bottom of the green box (panel G); (B) two vessels are seen in cross-section as circles, with hyperreflective borders and casting long shadows posteriorly. Deep horizontal hyperreflective lines are also seen, seemingly in isolation; (C) an adjacent section shows persistence of the circular vessel cross-sections and the anterior surface of a large and very deeply buried ODD accounting for the hyperreflective bands seen in panel B; (D) the consecutive circular cross-sections begin to form the 3-dimensional idea of tubular blood vessels and not a discrete lumpy ODD. Hyperreflective bands are seen on the lateral edges of the deep ODD; (E) the rightmost vessel becomes more oblong as the EDI-OCT transects a bifurcation. Only the anterior surface of the ODD is visible, with few hyperreflective bands; (F) the rightmost vessel has bifurcated into two smaller vessels. The deep ODD is barely visible, though its anterior surface is still hyperreflective; (G) the leftmost vessel bifurcates with one branch sectioned along its length; the rightmost vessels' branches are circular in cross-section and straddle the bifurcating left vessel. The surface of the deep ODD is no longer visible except for seemingly isolated hyperreflective bands. The ability to scroll through consecutive OCT images allows one to see whether a circular hyperreflective structure is a tube (blood vessel) or a lump (ODD), and allows one to see whether hyperreflective bands are associated with a neighboring ODD evident on an adjacent section or are truly isolated. ODD, optic disc drusen; EDI-OCT, enhanced depth imaging optical coherence tomography.

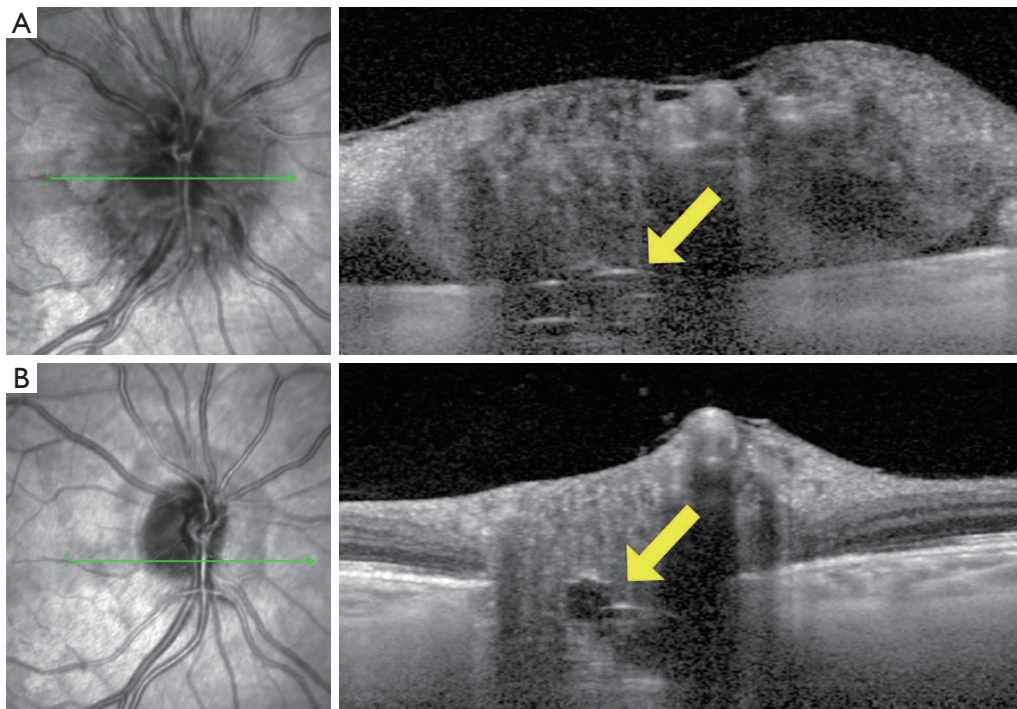


Figure 6 The appearance of ODD before and after resolution of optic disc edema in NAION: (A) infrared and EDI-OCT image of an optic disc during an acute episode of NAION, showing hyperreflective bands and a signal-poor core consistent with a buried ODD (arrow); (B) infrared and EDI-OCT image of the optic disc six months later, after resolution of optic disc edema, showing a more typical appearance of the buried ODD (arrow). ODD, optic disc drusen; EDI-OCT, enhanced depth imaging optical coherence tomography; NAION, non-arteritic ischemic optic neuropathy.

not be considered to be ODD without histopathological proof (32). In one study of clinically normal subjects (33), the prevalence of isolated hyperreflective bands reached 14.6%, far exceeding the 2% reported histopathological prevalence of ODD in the general population. Unlike more definite ODD, isolated hyperreflective bands are stereotyped, short, oriented perfectly perpendicular to the OCT beam, and often clustered together in a vertical stack. It is not clear whether isolated hyperreflective bands are also evident on SS-OCT, as there has only been one study comparing EDI-OCT to SS-OCT, in which isolated hyperreflective bands were not specifically examined (16). All authors studying these isolated hyperreflective bands have stressed the need for histopathological confirmation of what they may truly represent (6,21,32,33).

Mimics of ODD on OCT

PHOMS

Patients with ODD on EDI-OCT have sometimes also

been observed to have peripapillary hyperreflective ovoid mass-like structures (PHOMS) (Figures 3,4C,E,F,G). While some researchers have argued that these structures may represent superficial, early, or atypical ODD (34,35), the consensus now is that PHOMS are actually common EDI-OCT mimics of ODD, rather than true ODD (32). Various lines of evidence refute the theory of PHOMS being ODD: PHOMS do not autofluorescence; they are not visible on B-scan orbital ultrasonography; they are not visible on ophthalmoscopy despite their superficial location, except perhaps as pseudopapilledema; they are hyperreflective unlike all other ODD; and they are located in the peripapillary region of the disc, sometimes forming a “donut” shape around the optic disc. PHOMS are not unique to patients with true ODD; PHOMS have been found in papilledema from active idiopathic intracranial hypertension (and disappear when the papilledema resolves), anterior ischemic optic neuropathy, central retinal vein occlusion, papillitis, and even high myopia (36). Furthermore, histopathological studies of

papilledema (1,13,37) and ODD (1,3,10) have shown bulging or herniation of distended axons laterally into the regions where PHOMS are typically seen. Although their prominence and ovoid shape on OCT may misleadingly suggest ODD, PHOMS are now believed simply to be a nonspecific marker of axonal distention and crowding (6,36,38,39).

Retinal blood vessels

Another common mimic of ODD encountered with OCT are normal retinal blood vessels. Blood vessels appear in the inner, superficial layers of the optic disc and cast shadows on deeper structures (*Figures 3,4A,B,E,F,G,H*). Though the vessel interior may not be signal-poor to the same extent as ODD, the vessel has hyperreflective anterior and posterior borders, and can appear oval and drusenoid when imaged in cross-section (*Figure 4G*). Unlike ODD, blood vessels have paired hyperreflective bands (anterior and posterior) and not clustered ones, and the arteriole-venule pair often forms a distinctive “figure of eight” configuration in cross-section (*Figure 4A,B,F,H*). It is usually not difficult to distinguish a long tubular blood vessel from a discrete lumpy ODD deposit by simply scrolling through consecutive cross-sectional OCT images in order to grasp a structure’s 3-dimensional extent (*Figure 5*) (32).

Pediatric ODD

ODD are frequently buried and non-calcified in children, hampering detection via ophthalmoscopy, ultrasonography, FAF and CT scan (40). In these cases, EDI-OCT may be able to detect ODD earlier and more reliably than other modalities. It is unclear whether ODD are congenital or if they occur at an early stage of childhood. ODD have been detected in patients as young as age 4 (41), but two case reports of children followed for ODD noted normal appearing optic discs prior to presentation (42,43). In one case, elevated optic discs were found incidentally at age 8, with documentation of normal optic discs at age 4. Superficial ODD became visible at age 11 (43). In the second case, the optic discs were reported as unremarkable at age 2, but appeared elevated on routine follow up at age 5. No calcification was seen on CT at that time, but repeat CT at age 8 demonstrated calcification consistent with buried ODD. The ODD became visible on ophthalmoscopy in one eye at age 12 and the other at age 21 (42).

The Copenhagen Child Cohort 2000 Eye Study

detected ODD in 1.0% of children age 11–12 using EDI-OCT. An additional 0.8% of subjects were found to have hyperreflective bands, but were not considered to have definite ODD (44). Follow up data on this same cohort at age 16–17 detected ODD in 2.2% of re-examined children (45). This is higher than the previously reported prevalence in children of 0.37%, based on ophthalmoscopy alone (46), reflecting the improved detection rate of OCT. The updated prevalence is also strikingly similar to that reported in adult histopathologic studies (1.8–2.0%) (3,10), although no equivalent cross-sectional study using EDI-OCT has been conducted in an adult population.

Differentiating ODD from optic disc edema

Buried ODD may be difficult to differentiate from true optic disc edema on funduscopy, particularly in young children with limited cooperation. Early identification of ODD can prevent unnecessary, expensive, and invasive testing during investigation for papilledema. In one study, 19 of 34 children referred for papilledema were eventually diagnosed with ODD (47). When EDI-OCT is not available to allow direct visualization of ODD, non-EDI-OCT may provide clues to differentiate true optic disc edema from pseudoedema. RNFL analysis has demonstrated increased thickness in optic disc edema versus ODD (19,24,25), particularly nasally (48), although this is controversial (49). Normative values vary between manufacturers and devices, limiting the use of RNFL analysis as a diagnostic technique on individual patients. Thompson *et al.* found Bruch’s membrane opening (BMO) to be smaller in eyes with ODD than papilledema (1,542 *vs.* 1,894 μm) in a pediatric cohort (50). Children from the Copenhagen Child Cohort 2000 Eye Study with ODD also had a narrower scleral canal opening compared with controls (1,339 *vs.* 1,508 μm) (51). Again, a device-specific normative database would be required to use this as a diagnostic tool for individual patients. Furthermore, an adult study demonstrated larger scleral canal size in ODD eyes compared to controls (2,520 *vs.* 1,832 μm) (52). It is possible that the growth of ODD over time could cause outward displacement of Bruch’s membrane, leading to larger measurements of scleral canal size in adults (27). Therefore, scleral canal size may only be useful in differentiation of ODD from optic disc edema in children.

Vascular complications of ODD

ODD are associated with retinal vascular complications,

including choroidal neovascular membrane (CNVM), retinal vein occlusion and retinal artery occlusion (40,53). CNVMs associated with ODD tend to be juxtapapillary, occur more frequently in children, and have a good prognosis without treatment (7,53). ODD are also known to be associated with non-arteritic ischemic optic neuropathy (NAION) (54). In a retrospective review of 119 patients with NAION, the presence of bilateral ODD was found to be a significant risk factor for fellow eye involvement in younger patients (hazard ratio 2.78) (55). In patients presenting with NAION without systemic vascular risk factors, EDI-OCT can be used to investigate for ODD, both to help define the etiology and prognosticate risk to the fellow eye. ODD are detectable in the acute phase of optic disc edema, but may become more easily recognizable once the edema has resolved (*Figure 6*).

Longitudinal follow-up of ODD

Several case reports and one case series have followed patients with ODD for between 16 and 56 years (42-44,51), demonstrating the gradual change in ODD from buried to superficial and non-calcified to calcified (42-44). Once the ODD became superficial, there was no documented change in the number and size of visible ODD over a median of 56 years in 8 patients (51). The transition from buried to superficial ODD appears to occur in the first 2 decades of life, with no documented visible progression beyond age 16 in these reports (27,42-44). In a study of 50 children with ODD, 18% were visible in children age 7-10 and 37% were visible in children age 11-14 (46). Despite the lack of visible change, Malmqvist and colleagues documented progression of visual field loss, with a decrease in the area on Goldman perimetry by 27% with size 5 stimulus (6 eyes) and by 45% with size 1 stimulus (7 eyes) over 56 years (44). This progressive visual field loss could be related to continued axonal compression, but change in the non-visible ODD cannot be excluded as there are no long term studies using EDI-OCT to determine whether deeper ODD change over time. In one study, superficial ODD were shown to correlate with visual field defects and RNFL thinning more than buried ODD (26).

Conclusions

Because only a fraction of ODD are visible on ophthalmoscopy, particularly in children, advanced optic

disc imaging is often necessary to detect ODD. As there is currently no known treatment or prevention for ODD, the primary clinical utility of diagnosing ODD is to rule out other more dangerous causes of optic disc elevation. EDI-OCT is emerging as the single best imaging modality to evaluate ODD, and has a detection rate approaching that of cadaveric histopathological studies (10,45). Where it has been studied in comparison to other modalities, EDI-OCT detects cases of ODD missed by other modalities and does not miss cases picked up by these other modalities (21,22). In particular, EDI-OCT seems to surpass the existing gold standard of B-scan orbital ultrasound in its ability to detect ODD, and its extraordinarily high spatial resolution confers an added ability to determine the location, number, volume, and shape of ODD, even when small and deeply buried.

Visible ODD do not appear to change in adulthood, but little is known about the long-term stability of buried ODD. The association between hyperreflective bands and ODD is not yet confirmed, but promising data is being generated through longitudinal imaging. EDI-OCT has become the most important biomarker for evaluation and management of ODD with the potential to better understand when and how ODD form, and the mechanism underlying vision loss.

Acknowledgments

Funding: None.

Footnote

Provenance and Peer Review: This article was commissioned by the Guest Editors (Fiona Costello and Steffen Hamann) for the series “The Use of OCT as a Biomarker in Neuro-ophthalmology” published in *Annals of Eye Science*. The article has undergone external peer review.

Conflicts of Interest: Both authors have completed the ICMJE uniform disclosure form (available at <http://dx.doi.org/10.21037/aes.2019.12.03>). The series “The Use of OCT as a Biomarker in Neuro-ophthalmology” was commissioned by the editorial office without any funding or sponsorship. LLC D Bursztyn: Consultant for AbbVie, Consultant for Allergan. The authors have no other conflicts of interest to declare.

Ethical Statement: The authors are accountable for all aspects of the work in ensuring that questions related

to the accuracy or integrity of any part of the work are appropriately investigated and resolved.

Open Access Statement: This is an Open Access article distributed in accordance with the Creative Commons Attribution-NonCommercial-NoDerivs 4.0 International License (CC BY-NC-ND 4.0), which permits the non-commercial replication and distribution of the article with the strict proviso that no changes or edits are made and the original work is properly cited (including links to both the formal publication through the relevant DOI and the license). See: <https://creativecommons.org/licenses/by-nc-nd/4.0/>.

References

1. Tso MO. Pathology and pathogenesis of drusen of the optic nervehead. *Ophthalmology* 1981;88:1066-80.
2. Kapur R, Pulido JS, Abraham JL, et al. Histologic findings after surgical excision of optic nerve head drusen. *Retina* 2008;28:143-6.
3. Friedman AH, Gartner S, Modi SS. Drusen of the optic disc: a retrospective study in cadaver eyes. *Br J Ophthalmol* 1975;59:413.
4. Kelley JS. Autofluorescence of drusen of the optic nerve head. *Arch Ophthalmol* 1974;92:263-4.
5. Friedman AH, Beckerman B, Gold DH, et al. Drusen of the optic disc. *Surv Ophthalmol* 1977;21:373-90.
6. Palmer E, Gale J, Crowston JG, et al. Optic nerve head drusen: an update. *Neuro-ophthalmology* 2018;42:367-84.
7. Auw-Haedrich C, Staubach F, Witschel H. Optic disk drusen. *Surv Ophthalmol* 2002;47:515-532.
8. You QS, Xu L, Wang YX, et al. Prevalence of optic disc drusen in an adult Chinese population: the Beijing Eye Study. *Acta Ophthalmol* 2009;87:227-8.
9. Lorentzen SE. Drusen of the optic disk: a clinical and genetic study. *Acta Ophthalmol (Copenh)* 1966;Suppl 90:1-180.
10. Skougaard M, Heegaard S, Malmqvist L, et al. Prevalence and histopathological signatures of optic disc drusen based on microscopy of 1713 enucleated eyes. *Acta Ophthalmol* 2019. [Epub ahead of print].
11. Kurz-Levin MM, Landau K. A comparison of imaging techniques for diagnosing drusen of the optic nerve head. *Arch Ophthalmol* 1999;117:1045-9.
12. Roh S, Noecker RJ, Schuman JS, et al. Effect of optic nerve head drusen on nerve fiber layer thickness. *Ophthalmology* 1998;105:878-85.
13. Yi K, Mujat M, Sun W, et al. Imaging of optic nerve head drusen: improvements with spectral domain optical coherence tomography. *J Glaucoma* 2009;18:373-8.
14. Murthy RK, Storm L, Grover S, et al. In-vivo high resolution imaging of optic nerve head drusen using spectral-domain optical coherence tomography. *BMC Med Imaging* 2010;10:11.
15. Silverman AL, Tatham AJ, Medeiros FA, et al. Assessment of optic nerve head drusen using enhanced depth imaging and swept source optical coherence tomography. *J Neuroophthalmol* 2014;34:198-205.
16. Sato T, Mrejen S, Spaide RF. Multimodal imaging of optic disc drusen. *Am J Ophthalmol* 2013;156:275-282.e1.
17. Spaide RF, Koizumi H, Pozonni MC. Enhanced depth imaging spectral-domain optical coherence tomography. *Am J Ophthalmol* 2008;146:496-500.
18. Tsikata E, Verticchio Vercellin AC, Falkenstein I, et al. Volumetric measurement of optic nerve head drusen using swept-source optical coherence tomography. *J Glaucoma* 2017;26:798-804.
19. Skaat A, Muylaert S, Mogil RS, et al. Relationship between optic nerve head drusen volume and structural and functional optic nerve damage. *J Glaucoma* 2017;26:1095-100.
20. Malmqvist L, Lindberg AW, Dahl VA, et al. Quantitatively measured anatomic location and volume of optic disc drusen: an enhanced depth imaging optical coherence tomography study. *Invest Ophthalmol Vis Sci* 2017;58:2491-7.
21. Merchant KY, Su D, Park SC, et al. Enhanced depth imaging optical coherence tomography of optic nerve drusen. *Ophthalmology* 2013;120:1409-14.
22. Loft FC, Malmqvist L, Lindberg ASW, Hamann S. The influence of volume and anatomic location of optic disc drusen on the sensitivity of autofluorescence. *J Neuroophthalmol* 2019;39:23-7.
23. Katz BJ, Pomeranz HD. Visual field defects and retinal nerve fiber layer defects in eyes with buried optic nerve drusen. *Am J Ophthalmol* 2006;141:248-53.
24. Flores-Rodríguez P, Gili P, Martín-Rios MD. Sensitivity and specificity of time-domain and spectral-domain optical coherence tomography in differentiating optic nerve head drusen and optic disc oedema. *Ophthalmic Physiol Opt* 2012;32:213-21.
25. Casado A, Rebollada G, Guerrero L, et al. Measurement of retinal nerve fiber layer and macular ganglion cell-inner plexiform layer with spectral-domain optical coherence

- tomography in patients with optic nerve head drusen. *Graefes Arch Clin Exp Ophthalmol* 2014;252:1653-60.
26. Malmqvist L, Wegener M, Sander BA, Hamann S. Peripapillary retinal nerve fiber layer thickness corresponds to drusen location and extent of visual field defects in superficial and buried optic disc drusen. *J Neuroophthalmol* 2016;36:41-5.
 27. Malmqvist L, Li XQ, Eckmann CL et al. Optic disc drusen in children: The Copenhagen child cohort 2000 eye study. *J Neuroophthalmol* 2018;38:140-6.
 28. Erkkilä H. The central vascular pattern of the eyeground in children with drusen of the optic disc. *Albrecht Von Graefes Arch Klin Exp Ophthalmol* 1976;199:1-10.
 29. Vahlgren J, Malmqvist L, Ruelokke LL, et al. The angioarchitecture of the optic nerve head in patients with optic disc drusen. *Neuroophthalmology* 2019;44:5-10.
 30. Gaier ED, Rizzo JF 3rd, Miller JB, et al. Focal capillary dropout associated with optic disc drusen using optical coherence tomographic angiography. *J Neuroophthalmol* 2017;37:405-10.
 31. Cennamo G, Tebaldi S, Amoroso F, et al. Optical coherence tomography angiography in optic nerve drusen. *Ophthalmic Res* 2018;59:76-80.
 32. Malmqvist L, Bursztyn L, Costello F, et al. The Optic Disc Drusen Studies Consortium recommendations for diagnosis of optic disc drusen using optical coherence tomography. *J Neuroophthalmol* 2018;38:299-307.
 33. Ghassibi MP, Chien JL, Abumasmah RK, et al. Optic nerve head drusen prevalence and associated factors in clinically normal subjects measured using optical coherence tomography. *Ophthalmology* 2017;124:320-5.
 34. Traber GL, Weber KP, Sabah M, et al. Enhanced depth imaging optical coherence tomography of optic nerve head drusen: a comparison of cases with and without visual field loss. *Ophthalmology* 2017;124:66-73.
 35. Lee KM, Woo SJ, Hwang JM. Peripapillary ovoid mass-like structures: is it optic disc drusen or not? *J Neuroophthalmol* 2018;38:567-8.
 36. Malmqvist L, Sibony PA, Fraser CL, et al. Peripapillary ovoid hyperreflectivity in optic disc edema and pseudopapilledema. *Ophthalmology* 2018;125:1662-4.
 37. Paton L, Holmes G. The pathology of papilloedema: a historical study of sixty eyes. *Brain* 1911;33:389-432.
 38. Malmqvist L, Fraser C, Fraser JA, et al. RE: Traber et al.: Enhanced depth imaging optical coherence tomography of optic nerve head drusen: a comparison of cases with and without visual field loss. *Ophthalmology* 2017;124:e55-e56.
 39. Malmqvist L, Bursztyn L, Costello F, et al. Peripapillary hyperreflective ovoid mass-like structures: is it optic disc drusen or not? *J Neuroophthalmol* 2018;38:568-70.
 40. Chang MY, Pineles SL. Optic disc drusen in children. *Surv Ophthalmol* 2016;61:745-58.
 41. Erkkilä H. Clinical appearance of optic disc drusen in childhood. *Albrecht Von Graefes Arch Klin Exp Ophthalmol* 1975;193:1-18.
 42. Spencer TS, Katz BJ, Weber SW et al. Progression from anomalous optic discs to visible optic disc drusen. *J Neuroophthalmol* 2004;24:297-8.
 43. Frisén L. Evolution of drusen of the optic nerve head over 23 years. *Acta Ophthalmol* 2008;86:111-2.
 44. Malmqvist L, Lund-Andersen H, Hamann S. Long-term evolution of superficial optic disc drusen. *Acta Ophthalmol* 2017;95:352-6.
 45. Malmqvist L, Li XQ, Hansen MH, et al. Progression over five years of prelaminar hyperreflective lines to optic disc drusen in the Copenhagen Child Cohort 2000 Eye Study. *J Neuroophthalmol* 2019 (in press).
 46. Erkkilä H. Optic disc drusen in children. *Albrecht Von Graefes Arch Klin Exp Ophthalmol* 1973;189:1-7.
 47. Kovarik JJ, Doshi PN, Collinge JE et al. Outcome of pediatric patients referred for papilledema. *J AAPOS* 2015;19:344-8.
 48. Lee KM, Woo SJ, Hwang JM. Differentiation of optic nerve head drusen and optic disc edema with spectral-domain optical coherence tomography. *Ophthalmology* 2011;118:971-7.
 49. Kulkarni KM, Pasol J, Rosa PR et al. Differentiation mild papilledema and buried optic nerve head drusen using spectral domain optical coherence tomography. *Ophthalmology* 2014;121:959-63.
 50. Thompson AC, Bhatti MT and El-Dairi MA. Bruch's membrane opening on optical coherence tomography in pediatric papilledema and pseudopapilledema. *J AAPOS* 2018;22:38-43.e3.
 51. Malmqvist L and Hamann S. Photographic documentation of optic disc drusen over more than 50 years. *JAMA Ophthalmol* 2017;135:e165470.
 52. Floyd MS, Katz BJ, Digre KB. Measurement of the scleral canal using optical coherence tomography in patients with optic disc drusen. *Am J Ophthalmol* 2005;139:664-9.
 53. Duncan JE, Freedman SF and El-Dairi MA. The incidence of neovascular membranes and visual field defects from optic nerve head drusen in children. *J*

- AAPOS 2016;20:44-8.
54. Purvin V, King R, Kawasaki A et al. Anterior ischemic optic neuropathy in eyes with optic disc drusen. Arch Ophthalmol 2004;122:48-53.
55. Chang MY, Keltner JL. Risk factors for fellow eye involvement in nonarteritic anterior ischemic optic neuropathy. J Neuroophthalmol 2019;39:147-52.

doi: 10.21037/aes.2019.12.03

Cite this article as: Fraser JA, Bursztyn LLCD. Optical coherence tomography in optic disc drusen. Ann Eye Sci 2020;5:5.